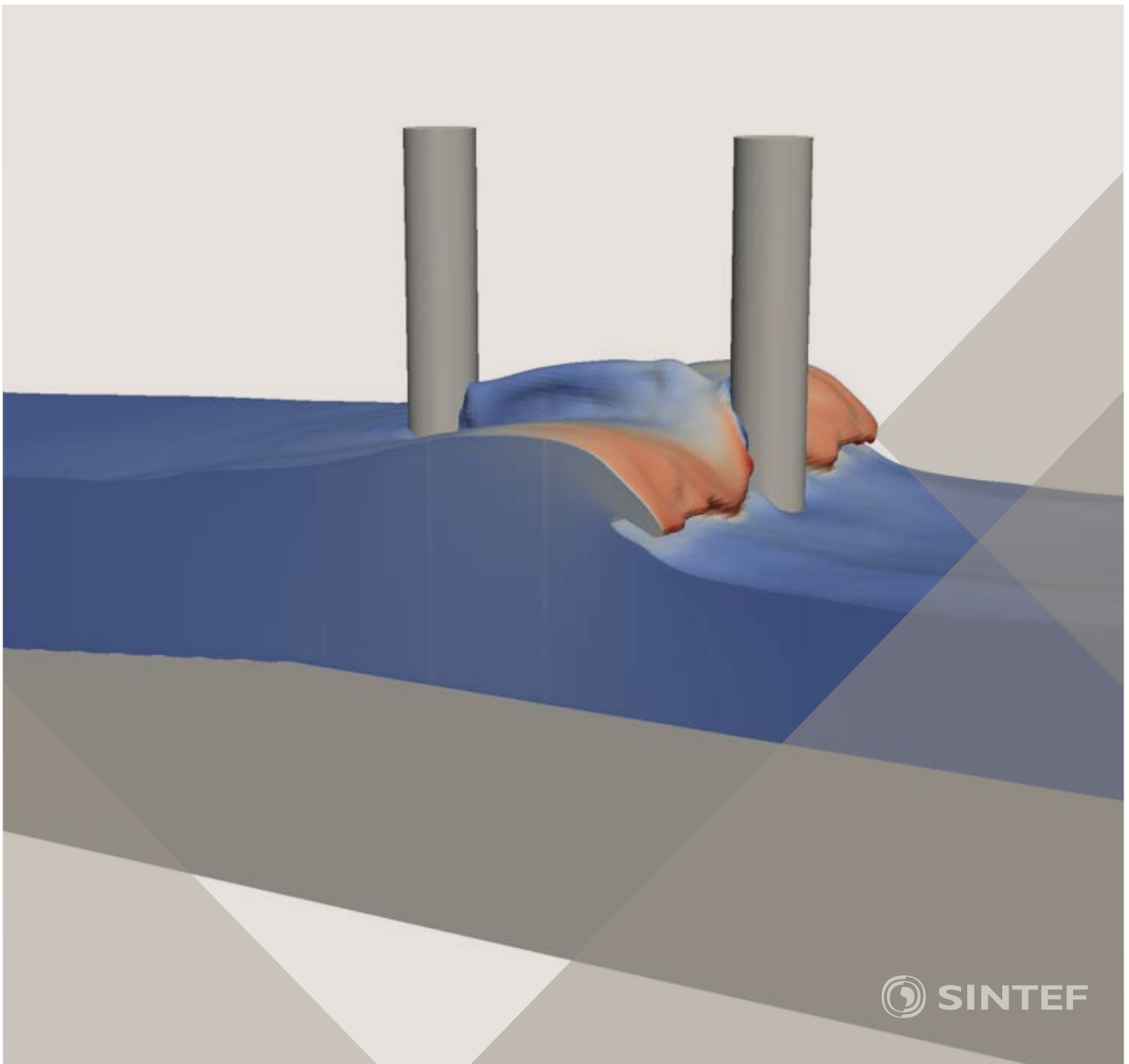


Proceedings of the 12th International Conference on
Computational Fluid Dynamics in the Oil & Gas,
Metallurgical and Process Industries

Progress in Applied CFD – CFD2017



SINTEF Proceedings

Editors:

Jan Erik Olsen and Stein Tore Johansen

Progress in Applied CFD – CFD2017

Proceedings of the 12th International Conference on Computational Fluid Dynamics
in the Oil & Gas, Metallurgical and Process Industries

SINTEF Academic Press

SINTEF Proceedings no 2

Editors: Jan Erik Olsen and Stein Tore Johansen

Progress in Applied CFD – CFD2017

Selected papers from 10th International Conference on Computational Fluid Dynamics in the Oil & Gas, Metallurgical and Process Industries

Key words:

CFD, Flow, Modelling

Cover, illustration: Arun Kamath

ISSN 2387-4295 (online)

ISBN 978-82-536-1544-8 (pdf)

© Copyright SINTEF Academic Press 2017

The material in this publication is covered by the provisions of the Norwegian Copyright Act. Without any special agreement with SINTEF Academic Press, any copying and making available of the material is only allowed to the extent that this is permitted by law or allowed through an agreement with Kopinor, the Reproduction Rights Organisation for Norway. Any use contrary to legislation or an agreement may lead to a liability for damages and confiscation, and may be punished by fines or imprisonment

SINTEF Academic Press

Address: Forskningsveien 3 B
 PO Box 124 Blindern
 N-0314 OSLO

Tel: +47 73 59 30 00

Fax: +47 22 96 55 08

www.sintef.no/byggforsk

www.sintefbok.no

SINTEF Proceedings

SINTEF Proceedings is a serial publication for peer-reviewed conference proceedings on a variety of scientific topics.

The processes of peer-reviewing of papers published in SINTEF Proceedings are administered by the conference organizers and proceedings editors. Detailed procedures will vary according to custom and practice in each scientific community.

PREFACE

This book contains all manuscripts approved by the reviewers and the organizing committee of the 12th International Conference on Computational Fluid Dynamics in the Oil & Gas, Metallurgical and Process Industries. The conference was hosted by SINTEF in Trondheim in May/June 2017 and is also known as CFD2017 for short. The conference series was initiated by CSIRO and Phil Schwarz in 1997. So far the conference has been alternating between CSIRO in Melbourne and SINTEF in Trondheim. The conferences focuses on the application of CFD in the oil and gas industries, metal production, mineral processing, power generation, chemicals and other process industries. In addition pragmatic modelling concepts and bio-mechanical applications have become an important part of the conference. The papers in this book demonstrate the current progress in applied CFD.

The conference papers undergo a review process involving two experts. Only papers accepted by the reviewers are included in the proceedings. 108 contributions were presented at the conference together with six keynote presentations. A majority of these contributions are presented by their manuscript in this collection (a few were granted to present without an accompanying manuscript).

The organizing committee would like to thank everyone who has helped with review of manuscripts, all those who helped to promote the conference and all authors who have submitted scientific contributions. We are also grateful for the support from the conference sponsors: ANSYS, SFI Metal Production and NanoSim.

Stein Tore Johansen & Jan Erik Olsen



Organizing committee:

Conference chairman: Prof. Stein Tore Johansen

Conference coordinator: Dr. Jan Erik Olsen

Dr. Bernhard Müller

Dr. Sigrid Karstad Dahl

Dr. Shahriar Amini

Dr. Ernst Meese

Dr. Josip Zoric

Dr. Jannike Solsvik

Dr. Peter Witt

Scientific committee:

Stein Tore Johansen, SINTEF/NTNU

Bernhard Müller, NTNU

Phil Schwarz, CSIRO

Akio Tomiyama, Kobe University

Hans Kuipers, Eindhoven University of Technology

Jinghai Li, Chinese Academy of Science

Markus Braun, Ansys

Simon Lo, CD-adapco

Patrick Segers, Universiteit Gent

Jiyuan Tu, RMIT

Jos Derksen, University of Aberdeen

Dmitry Eskin, Schlumberger-Doll Research

Pär Jönsson, KTH

Stefan Pirker, Johannes Kepler University

Josip Zoric, SINTEF

CONTENTS

PRAGMATIC MODELLING	9
On pragmatism in industrial modeling. Part III: Application to operational drilling	11
CFD modeling of dynamic emulsion stability	23
Modelling of interaction between turbines and terrain wakes using pragmatic approach	29
FLUIDIZED BED	37
Simulation of chemical looping combustion process in a double looping fluidized bed reactor with cu-based oxygen carriers.....	39
Extremely fast simulations of heat transfer in fluidized beds.....	47
Mass transfer phenomena in fluidized beds with horizontally immersed membranes	53
A Two-Fluid model study of hydrogen production via water gas shift in fluidized bed membrane reactors	63
Effect of lift force on dense gas-fluidized beds of non-spherical particles	71
Experimental and numerical investigation of a bubbling dense gas-solid fluidized bed	81
Direct numerical simulation of the effective drag in gas-liquid-solid systems	89
A Lagrangian-Eulerian hybrid model for the simulation of direct reduction of iron ore in fluidized beds.....	97
High temperature fluidization - influence of inter-particle forces on fluidization behavior	107
Verification of filtered two fluid models for reactive gas-solid flows	115
BIOMECHANICS.....	123
A computational framework involving CFD and data mining tools for analyzing disease in carotid artery	125
Investigating the numerical parameter space for a stenosed patient-specific internal carotid artery model.....	133
Velocity profiles in a 2D model of the left ventricular outflow tract, pathological case study using PIV and CFD modeling.....	139
Oscillatory flow and mass transport in a coronary artery.....	147
Patient specific numerical simulation of flow in the human upper airways for assessing the effect of nasal surgery.....	153
CFD simulations of turbulent flow in the human upper airways	163
OIL & GAS APPLICATIONS	169
Estimation of flow rates and parameters in two-phase stratified and slug flow by an ensemble Kalman filter	171
Direct numerical simulation of proppant transport in a narrow channel for hydraulic fracturing application	179
Multiphase direct numerical simulations (DNS) of oil-water flows through homogeneous porous rocks	185
CFD erosion modelling of blind tees	191
Shape factors inclusion in a one-dimensional, transient two-fluid model for stratified and slug flow simulations in pipes	201
Gas-liquid two-phase flow behavior in terrain-inclined pipelines for wet natural gas transportation	207

NUMERICS, METHODS & CODE DEVELOPMENT	213
Innovative computing for industrially-relevant multiphase flows	215
Development of GPU parallel multiphase flow solver for turbulent slurry flows in cyclone.....	223
Immersed boundary method for the compressible Navier–Stokes equations using high order summation-by-parts difference operators	233
Direct numerical simulation of coupled heat and mass transfer in fluid-solid systems	243
A simulation concept for generic simulation of multi-material flow, using staggered Cartesian grids.....	253
A cartesian cut-cell method, based on formal volume averaging of mass, momentum equations.....	265
SOFT: a framework for semantic interoperability of scientific software	273
 POPULATION BALANCE	 279
Combined multifluid-population balance method for polydisperse multiphase flows	281
A multifluid-PBE model for a slurry bubble column with bubble size dependent velocity, weight fractions and temperature.....	285
CFD simulation of the droplet size distribution of liquid-liquid emulsions in stirred tank reactors	295
Towards a CFD model for boiling flows: validation of QMOM predictions with TOPFLOW experiments	301
Numerical simulations of turbulent liquid-liquid dispersions with quadrature-based moment methods.....	309
Simulation of dispersion of immiscible fluids in a turbulent couette flow	317
Simulation of gas-liquid flows in separators - a Lagrangian approach.....	325
CFD modelling to predict mass transfer in pulsed sieve plate extraction columns	335
 BREAKUP & COALESCENCE	 343
Experimental and numerical study on single droplet breakage in turbulent flow	345
Improved collision modelling for liquid metal droplets in a copper slag cleaning process	355
Modelling of bubble dynamics in slag during its hot stage engineering.....	365
Controlled coalescence with local front reconstruction method	373
 BUBBLY FLOWS	 381
Modelling of fluid dynamics, mass transfer and chemical reaction in bubbly flows	383
Stochastic DSMC model for large scale dense bubbly flows.....	391
On the surfacing mechanism of bubble plumes from subsea gas release.....	399
Bubble generated turbulence in two fluid simulation of bubbly flow	405
 HEAT TRANSFER	 413
CFD-simulation of boiling in a heated pipe including flow pattern transitions using a multi-field concept	415
The pear-shaped fate of an ice melting front	423
Flow dynamics studies for flexible operation of continuous casters (flow flex cc).....	431
An Euler-Euler model for gas-liquid flows in a coil wound heat exchanger.....	441
 NON-NEWTONIAN FLOWS.....	 449
Viscoelastic flow simulations in disordered porous media	451
Tire rubber extrudate swell simulation and verification with experiments	459
Front-tracking simulations of bubbles rising in non-Newtonian fluids.....	469
A 2D sediment bed morphodynamics model for turbulent, non-Newtonian, particle-loaded flows.....	479

METALLURGICAL APPLICATIONS.....	491
Experimental modelling of metallurgical processes	493
State of the art: macroscopic modelling approaches for the description of multiphysics phenomena within the electroslag remelting process	499
LES-VOF simulation of turbulent interfacial flow in the continuous casting mold	507
CFD-DEM modelling of blast furnace tapping	515
Multiphase flow modelling of furnace tapholes	521
Numerical predictions of the shape and size of the raceway zone in a blast furnace.....	531
Modelling and measurements in the aluminium industry - Where are the obstacles?	541
Modelling of chemical reactions in metallurgical processes.....	549
Using CFD analysis to optimise top submerged lance furnace geometries	555
Numerical analysis of the temperature distribution in a martensitic stainless steel strip during hardening.....	565
Validation of a rapid slag viscosity measurement by CFD.....	575
Solidification modeling with user defined function in ANSYS Fluent.....	583
Cleaning of polycyclic aromatic hydrocarbons (PAH) obtained from ferroalloys plant.....	587
Granular flow described by fictitious fluids: a suitable methodology for process simulations	593
A multiscale numerical approach of the dripping slag in the coke bed zone of a pilot scale Si-Mn furnace.....	599
INDUSTRIAL APPLICATIONS	605
Use of CFD as a design tool for a phosphoric acid plant cooling pond	607
Numerical evaluation of co-firing solid recovered fuel with petroleum coke in a cement rotary kiln: Influence of fuel moisture	613
Experimental and CFD investigation of fractal distributor on a novel plate and frame ion-exchanger	621
COMBUSTION	631
CFD modeling of a commercial-size circle-draft biomass gasifier.....	633
Numerical study of coal particle gasification up to Reynolds numbers of 1000.....	641
Modelling combustion of pulverized coal and alternative carbon materials in the blast furnace raceway	647
Combustion chamber scaling for energy recovery from furnace process gas: waste to value	657
PACKED BED.....	665
Comparison of particle-resolved direct numerical simulation and 1D modelling of catalytic reactions in a packed bed	667
Numerical investigation of particle types influence on packed bed adsorber behaviour	675
CFD based study of dense medium drum separation processes	683
A multi-domain 1D particle-reactor model for packed bed reactor applications.....	689
SPECIES TRANSPORT & INTERFACES	699
Modelling and numerical simulation of surface active species transport - reaction in welding processes	701
Multiscale approach to fully resolved boundary layers using adaptive grids.....	709
Implementation, demonstration and validation of a user-defined wall function for direct precipitation fouling in Ansys Fluent.....	717

FREE SURFACE FLOW & WAVES	727
Unresolved CFD-DEM in environmental engineering: submarine slope stability and other applications.....	729
Influence of the upstream cylinder and wave breaking point on the breaking wave forces on the downstream cylinder	735
Recent developments for the computation of the necessary submergence of pump intakes with free surfaces	743
Parallel multiphase flow software for solving the Navier-Stokes equations	752
PARTICLE METHODS	759
A numerical approach to model aggregate restructuring in shear flow using DEM in Lattice-Boltzmann simulations	761
Adaptive coarse-graining for large-scale DEM simulations.....	773
Novel efficient hybrid-DEM collision integration scheme.....	779
Implementing the kinetic theory of granular flows into the Lagrangian dense discrete phase model.....	785
Importance of the different fluid forces on particle dispersion in fluid phase resonance mixers	791
Large scale modelling of bubble formation and growth in a supersaturated liquid.....	798
FUNDAMENTAL FLUID DYNAMICS	807
Flow past a yawed cylinder of finite length using a fictitious domain method	809
A numerical evaluation of the effect of the electro-magnetic force on bubble flow in aluminium smelting process.....	819
A DNS study of droplet spreading and penetration on a porous medium.....	825
From linear to nonlinear: Transient growth in confined magnetohydrodynamic flows.....	831

A MULTISCALE NUMERICAL APPROACH OF THE DRIPPING SLAG IN THE COKE BED ZONE OF A PILOT SCALE SI-MN FURNACE

Sebastien LETOUT^{1*}, Arne-Peter RATVIK², Merete TANGSTAD¹, Stein-Tore JOHANSEN²,
Jan-Erik OLSEN²

¹NTNU Department of Materials Science and Engineering, 7491 Trondheim, NORWAY

²SINTEF Materials and Chemistry, 7465 Trondheim, NORWAY

* E-mail: sebastien.letout@ntnu.no

ABSTRACT

The Si-Mn alloy process production in submerged arc furnaces (SAF) is investigated. The aim of the studies currently in progress is an enhancement of the knowledge about the key reactions and the mass transport phenomenon related to the metal production. Some small scale experiments on raw materials and bigger pilot scale experiments are done to understand local kinetic and its extension to real condition production furnaces. As it is impossible to observe what is happening in the core of the furnace during operation, excavation of the pilot scale furnace are realised after operations. Based on bibliographical description of similar processes, observations and species analyses after excavation, a numerical simulation is currently in development to test the hypothesis formulated about the internal behaviour of the furnace. As it is difficult to model the complex entire furnace, the work presented here is focusing on what are the phenomenas inside the coke bed, in the dripping zone where the slags flow around the carbon particles before reaching the bottom of the furnace. The thrickling of the slags across the coke bed can be evaluated by a simulation of the droplets finding their path by gravity through the packing of carbon particles. This study has to be very local in space and time, but can give some useful informations such as velocities and drag force. At a larger scale (ie furnace scale), the coke bed particles are modelled by a granular phase in an eulerian-eulerian representation where the slag phase flow interact in the same way as in the local study. The slag is found to flow across the coke bed under the form of droplets of a maximum diameter of 10mm. The apparent velocity of the fluid is about 0,12 m/s. However the residence time of the droplets is longer due to the liquid trapped along the coke bed.

Keywords: Packed bed, Granular flow, Free surface flow, Multi-phase mass transfer, Multiscale .

NOMENCLATURE

Greek Symbols

ρ Mass density, [kg/m^3]
 μ Dynamic viscosity, [kg/ms]
 α Surface tension, [kg/s^2]

Latin Symbols

u Averaged volume Velocity, [m/s].
K Momentum exchange Coefficient, [$1/s$].
F Volumic Force, [$kg/m^2.s^{-2}$].
g Gravitational Acceleration, [m/s^{-2}].

ΔH Reaction enthalpie, [J/mol].
q Heat flux, [$J/m^2.s$].
h Convective heat transfer coefficient, [$J/m^2.s.K$].
rr Reaction rate, [$mol/m^3.s$].
T Temperature, [K].
A_{dst} Area density, [m^2/m^3].

Sub/superscripts

p particle.
s slag.
g gas.
eq equilibrium.

INTRODUCTION

In the steel industry, manganese is an important element needed in order to produce specific grades of steel, ranging from materials having a great toughness, a high strength or containing low carbon. Manganese is added into the steel production furnace in the form of alloys and mainly ferroalloys. Silico-manganese, also called SiMn is another alloy which is privileged in the production of silicon and manganese containing steel.

The major part of SiMn is produced in submerged arc furnace (SAF) by carbothermic reduction of oxidic raw materials. An experimental effort has been conducted these last years at NTNU, operating a pilot scale SAF to investigate the parameters limiting the conversion of slag into metal alloy. Currently about 35 % of the mass is tapped from the production furnace as a metal, leaving the 65% remaining in a slag form.

To facilitate the understanding of the furnace, a modeling effort of the furnace is conducted in order to give different scenarios conducting to the conversion of slag into metal. Hypothesis has to be made to describe the furnace, and, to reduce the complexity of the problem, the whole problem has been split into more elementary part.

This paper is focusing on the modeling strategy used to depict one part, identified as the dripping part of the furnace.

FURNACE DESCRIPTION

The pilot scale furnace (Ringdalen and Tangstad, 2013) is a cylindrical container of 450 mm of inner diameter and the charge height is around 700mm. The furnace is filled with ores and the charge is always maintained up to its maximum height level during operations. There are two electrodes; a top one situated in the furnace and a bottom one situated under the furnace. Their role is to bring thermal energy to the particles due to ohmic dissipation inside the conducting material which is mostly carbon particles.

The furnace is usually reported to be composed of two parts that is the pre-reduction zone and the reduction zone. The pre-reduction zone is the upper part of the furnace where the ores are reduced (FeO) or pre-reduced (Mn_3O_4 , Mn_2O_3 , MnO_2). This zone is heated by the exothermic pre-reduction reactions as well as by the hot flux of CO gas ascending from the reduction zone which is at the same time a reactant in the pre-reduction reactions (figure 1). The reduction zone is located on the bottom half of the furnace. In this zone, due to Joule dissipation in the carbon particles, the ores are melted and reduced into metal by carbo-reduction. The general layout of the reducing steps and the kinetic associated is not yet well known and are the object of the current investigations. Poor pre-reduction of the ores as well as limited ores reduction lead to partial conversion of the slag into metal.

As the core of the metal production process is happening in the reduction zone, it is interesting to investigate this zone more deeply.

PHYSIC OF THE PROCESS

The process involves various different physical phenomena which are coupled together such as electricity, thermodynamics, turbulent hydrodynamics, heat radiation and chemical reactions. The complexity of the interdependency of these phenomena both in a mathematical way and due to the existence of different zones inside the furnace lead to challenging modeling where some choices have to be done.

Phases At least 4 phases have to be taken into account that is the gas phase, the solid phase and two liquid phases. The oxides form the liquid slag phase, whereas the reduced oxides are combined together into another liquid phase which is the metal phase. The pre-reduction zone is mainly constituted of solid and gas whereas in the reduction zone, the two liquids are flowing through a bed of solid particles.

Species The number of species present can be quite large due to the wide variety of ore materials used. In those materials some elements participate only in the slag phase (CaO , MgO , BaO , Al_2O_3), as they seem not to be involved into the reacting system of metal production. The solid material are mainly Mn_xO_y , SiO_2 , and the carbon represented as coke. The fluid species can be classified in two types that is the oxides and the metallic compounds. The slag components taking part of the reaction are mainly SiO_2 and MnO whereas the metallic component are by order of importance Mn, Fe and Si. The gas phase is composed of CO and CO_2 , but only CO is present into the whole furnace.

In this paper we focus on the way the melting ores are dripping on carbon particles.

DATAS AVAILABLE TO PROCESS THE MODELING.

Due to the temperature, the size, and the opacity of the system, it is difficult to monitor internal parameters such as the

temperature, the flow rate, or the reduction rate in the furnace.

The data available during a run are mostly external parameters that is the power supplied to the installation and the variation of resistance measured in between the electrodes, the quantity of molten slag and metal collected every 30 min, the temperature of the tapped liquid and the analysis of this liquid components after operations.

At the end of the operations the furnace is cooled down and the void areas are filled with epoxy. A slice along the diameter of the furnace is realised. This slice, called the excavation plate, gives us a picture of the furnace at the instant when the electrical power is shutdown. The informations extracted from it can help us to understand the internal process during operations. The hypothesis made is that no reduction happen during the cooling process as not enough power is supplied to continue the reduction. From the excavation of the furnace some informations about the solid phase packing can be extracted, as well as the composition of some phases remaining. According to these excavations, it seems that 90% of the reduction happen on a thin layer situated at the top of the reduction zone, at the interface with the pre-reduction zone, where the reacting ores, already liquid are reduced. The 10% remaining reduction should happen in the coke bed by dripping down through it.

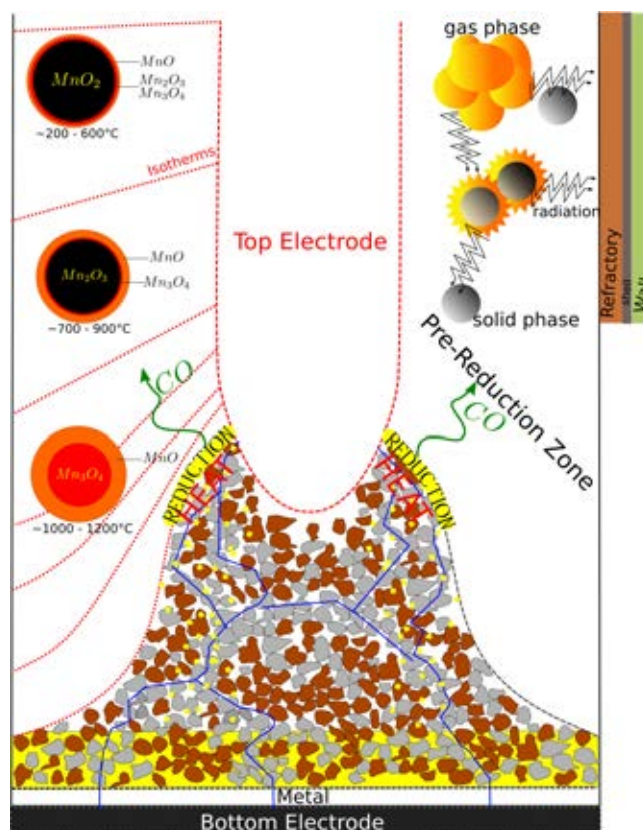


Figure 1: Scheme of the Si-Mn pilot-scale furnace

COKE BED, THE DRIPPING ZONE

As the phenomenons explaining that most of the reduction operations happen on the top of the coke bed are not yet well identified and just hypothesis, it is difficult to model the entire coke bed as a whole. Indeed the slag in liquid state has to stay long enough on the top of the coke bed to be reduced without flowing in the down part of the coke bed.

To decouple the problem, we focus on the way the liquid slag flow through the coke bed (see figure 1). This zone is referred to the dripping zone. It is the zone where the slag flow by gravity around the carbon particles. The description we depict now is similar to the one observed in the blast furnace where the dripping zone is described as a zone of great importance to the mass transfer of elements (Husslage *et al.*, 2005).

To study this zone we are using two different numerical models involving two different scales :

- one local model where the interstitial space between carbon particles is meshed, and where the interface of the flowing fluid slag is tracked with the help of the Volume of Fluid method
- one global model where the phases fractions are tracked in each cells with the Euler-Euler method. In this model, the cells are bigger than the inter-poral space and the whole dripping zone is modeled.

In the dripping zone the temperature is assumed to be maintained at a value of about 1873 K. It is the temperature measured of the tapped metal, and just above the temperature of reduction of the ores.

THE TWO SCALES MODEL

The local model

This part of the calculations referred to the local model are done in order to give a representation about the intensity and the configuration of the dripping slag into the coke bed.

We consider a 2D box representing some carbon particles digitized from the real geometry (figure 2). In this box only the poral space around the carbon particles is meshed, using the snappyHexMesh tool of OpenFoam 4.1 (OF4.1).

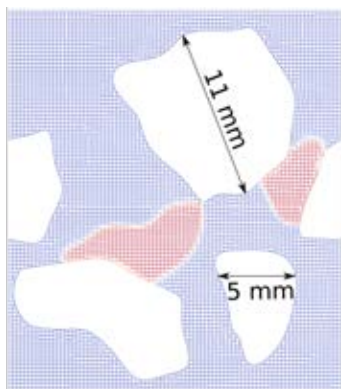


Figure 2: 2D box for slag droplet simulation

This box have to be small enough to permit a fine meshing of the poral space and large enough to contain at least some droplets free to move.

The solid fraction in the box is representative of the average solid fraction of the real packing in the pilot scale experiment. The slag phase is introduced by initializing its phase fraction to 1 into a geometrical zone representing the desired quantity of liquid, This liquid is initially at rest (zero velocity), and flows by gravity.

Periodic boundary conditions are used on top and bottom of the box, and non matching cyclic boundary conditions are used on the right and left side of the box.

The method used is the Volume Of Fluid method which solve all the phases with one set of conservation equations. The

solver is the interFlow solver based on interFoam version of OF 4.1.

In this solver, the interface reconstruction algorithm used is the recent isoAdvector algorithm (Roenby *et al.*, 2016), which oppositely to MULES, use geometrical interface reconstruction and advection instead of algebraic interface compression. This algorithm has been found to be more accurate in interface advection and reducing splashing of small parts of the volume fraction out of the main fluid flow. The performance of the algorithm is also very good in comparison to others geometrical reconstruction algorithm. Additionally the advection of the interface is almost not affected by the type and shape of cell used.

The solver is modified to introduce the gravity field into the momentum equation instead of the pressure equation, to avoid problems due to the non periodicity of the pressure field. The average slag velocity in the box is calculated with the velocity of the liquid phase along the dripping path of the slag. The volume of fluid reported divided by the height of the box and the final velocity, gives us the flow rate obtained when the slag reaches the bottom of the coke bed.

The goal of this calculation is to depict the behaviour of the slag when the flowrate calculated at the bottom of the coke bed is similar to the one deduced from the quantity of liquid obtained from each tapping of the pilot-scale experiment. This calculation is done iteratively by correcting the quantity of liquid introduced and the size of the simulation box until reaching some result in accordance with the experimental quantities obtained.

The hypothesis done during the calculation is that the slags are flowing homogeneously in the whole dripping zone and that the flow rate stay constant during all the process. The thickness of the droplets is estimated as being the average of the diameter of the flowing droplets considered. This study can be completed by taking into account the variation of the viscosity, surface tension, density and contact angle along the path, due to composition variation. As it is still a bit difficult to obtain the correct informations into both spatial variations of composition and properties evolutions related to these composition variation, the properties have been, in this attempt, kept constant.

This averaged velocity of the dripping slag has been reinterpreted in terms of drag coefficient of the coke bed :

$$F_{drag} = \alpha_s \rho_s (\mathbf{u}_p - \mathbf{u}_s) K_{p-s} + \alpha_s \rho_s (\mathbf{u}_g - \mathbf{u}_s) K_{g-s} = \alpha_s \rho_s \mathbf{g}$$

If we consider that there is no drag interaction between the gas and the slag phase and that the solid particles are not moving, we can then estimate the value of K_{p-s} with the expression $K_{p-s} = \mathbf{g}/u_s$. We can also deduce an order of size of the droplets by following the liquid phase in spaces without particles where the droplets are not combined together. Both datas can be used in a large scale modeling which will be presented in the next part.

The physical properties used to calculate the flow are based on the composition of the slag tapped after experiment. These properties are summarized in table 2 for an average slag composition obtained over several tapping given in 1.

Table 1: Slag composition (mass %) at the temperature T=1778K

Temperature	MnO	SiO ₂	CaO	MgO	Al ₂ O ₃
1778	21	39	19	8	13

Table 2: Physical properties of the slag whose composition is given in table 1

$\rho(kg.m^{-3})$	$\mu(Pa.s)$	$\sigma(N.m^{-1})$	θ	dynamic θ
3280	0.1	0.49	125	± 10

The global model

The Euler-Euler model of Fluent 17.2 is used to represent the dripping part of the whole furnace. This model offer the possibility to study a process on a large scale geometry. This model has been used to simulate several complex processes involving several phases and reactions. In metal production it has been used to simulate the trends of the silicon production process in an industrial configuration (Darmana *et al.*, 2012). In this model particle, liquids and gas phases are present in each cell. The phase fraction of the phases are tracked as well as their averaged velocity and temperature in each cell. Only one pressure field is calculated for all the phases, and the turbulent quantities k and ϵ are calculated for the mixture. The evolution of these continuous fields are calculated with the help of correlations to describe the inter-phase interaction inside the cells. These terms are added as source terms in the fluid flow equations (momentum and/or energy) of each phase. The study is axi-symmetric.

Solid phase The granular model is used to model the coke particles. The coke bed is represented as a packed bed with no velocity. The solid phase fraction is taken as the same as the one used in the local model (0.39). The size of the particles is also taken as representative of the coke bed (0.01 m).

Liquid phase The main parameter of the liquid phase is the size of the droplets flowing through the solid phase. The droplet size is assumed to be homogeneous in the whole furnace and the value is estimated from the calculations of the local model. The phase fraction in the domain is calculated from the imposed boundary conditions.

Gas phase The gas phase is the main or continuous phase which means that its phase fraction is calculated with the space non occupied by the other phases following $\alpha_{solid} + \alpha_{liquid} + \alpha_{gas} = 1$.

Geometry The geometry boundary are sketched from :

1. The walls of the furnace for the down and side boundary
2. The shape of the reduction zone determined from the excavation plate of the furnace.

The shape of the reduction zone can be located as the fictive boundary separating the zones with different solid composition. On the upper part a mix of solid coke and ore particles can be observed whereas on the lower part there is just solid coke remaining. The mesh generated with the Delaunay algorithm for quad (Remacle *et al.*, 2010) of the GMSH utility, is represented on figure 3.

Boundary conditions The fluid is entering the top part of the coke bed near the electrode, and the fluid is free to leave the coke bed (pressure outlet conditions) on both the lower part and the upper part of the coke bed (figure 3). The velocity inlet conditions are set in a way to respect the global flowrate of the experiment. The velocity is set at a similar value as the main value wanted into the coke bed, and the inlet phase fraction is adapted to this value.

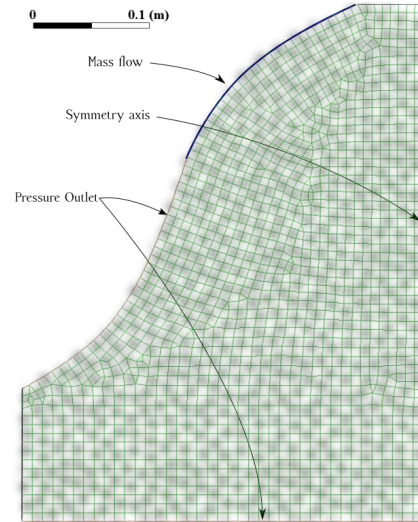


Figure 3: Geometry and mesh of the coke bed zone

Drag coefficient For the calculations of the drag coefficient between fluids the Schiller-Naumann correlation is used. For the drag interaction between the liquid and the solid, the K_{p-s} coefficient calculated previously and adapted to the dimensions required by the equation solved by Fluent ($kg.m^{-3}.s^{-1}$) is used.

RESULTS

Local model

The VOF model gives us several informations about the distribution of the droplets into the coke bed.

First, small droplets (diameter $< 9mm$) will flow quickly in places where the pore size is superior to their size. Depending on their velocity these droplets will go through smaller interpores. If the smaller interpore zone is smaller than the droplet diameter, and its inertia is not sufficient to cross the obstacle, then the droplet will get stuck. These droplets may fragment into smaller droplets when they impact a bigger particle with a high velocity (0.5 m/s), but usually due to the high surface tension and the friction along the coke bed, these droplets rarely split.

The high density (3 times higher than water), and the relatively low dynamic viscosity (comparable to olive oil) permit the slag phase to flow easily into the coke bed. Oppositely, the contact angle and the high surface tension oppose a resistance when it comes to zone with smaller pore dimensions.

Big droplets (diameter $> 10mm$) split in smaller droplets during their trickling path through the coke bed. The dynamic of the obtained droplets depends on the size of these droplets. As long as the smallest pores between particles is not filled with slag, the droplets will partially attach to the carbon particles which leads to a non steady flow rate, and a residence time of a droplet which vary at the beginning of the simulation. As these poral spaces of the coke bed are filled

with slag, we have a continuous process which begin, one droplet pushing the precedent droplet out to feel the cavity or to extract the totality of the fluid, releasing each time new droplets. The size and the dynamic of the new droplet depend on the quantity of liquid extracted from the cavity.

In this pseudo stationary regime the movement of fluid is estimated to be around 0.12 m/s with velocities ranging from 0m/s for the droplets trapped into the coke bed up to about 0.5 m/s during (free fall of some small droplets). The velocity of the droplets vary depending on how many filled cavities are met along the droplet path inside the coke bed. If we consider that the liquid pushed out of the cavity is the continuity of the one pushing the liquid then the velocity of one bubble of a diameter of 9 mm is about 0.12 m/s. The final size of the droplet at the bottom of the furnace does not depend directly of the size of the initial droplet but also of the quantity of liquid trapped into the pores. If the size of droplets stemming from the top of the coke bed is stationary then the size of a droplet trapped is about the same size and the size of the bubble released is also approximatively the same.

The wetting of the particles is a key parameter to determine the contact area between the slag and the solid particles. It depends on the physical properties of the fluid, in particular the contact angle, but also on the geometry of the particles and the interstitial space where the droplets are trapped. The scarcity of the droplets flowing through the coke bed and the high value of the contact angle explain that only a few part of the coke surface is wet by the slag in the dripping zone.

Global model

Introducing the correct order of magnitude of the particle size, coke bed void fraction and drag coefficient permit to simulate an averaged situation which is representative of our local simulation. The droplets of the predetermined size (4 mm in our simulations) flow in a coke bed at the approximate velocity of 0.1 m/s. This lead to a distribution of the phase fraction given by the calculation on figure 5. This model as such does not give more informations as it reproduces in a modeled way the results obtained with the local model.

The idea behind the use of this model is to add an energy balance calculation in the system by choosing the appropriate boundary conditions, energy sources and energy consumption inside the coke bed. This needs an accurate description of the thermo-physical properties of the system, electrical power released and of the kinetic of the reaction system. A first attempt has been made in this direction using the simplified system

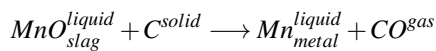


Figure 4: 3-6 mm droplets flowing along coke particles

involving just one component in each phase. The subscript specify the liquid phase whereas the superscript specify the physical state of the compound. The slag phase is composed of MnO, the metal phase of Mn, the solid phase is made of carbon and the gas phase is composed of CO. This means that in contact with carbon our slag phase transform into the metal phase. The reaction is endothermic, needing an external energy source to supply thermal power to the system.

The kinetics of the process is still in investigation, and, in this attempt we used a heat transfer correlation, the Gunn correlation to estimate the heat transfer coefficient h between the carbon phase and the slag phase. The reaction is temperature driven and the kinetics is based on the heat flux received by the material : $rr = A_{dst} \cdot q / \Delta H$ with $q = h(T_p - T_{eq})$. The value of the area concentration A_{dst} can be use to model the surface of contact between slag droplets and coke particles available for chemical reactions.

In the figure 6 we can see the calculated reaction rate of our implementation. The results are homogeneous on most of the part of the furnace, and a bit higher on the top zone of the furnace where the fluid is slower.

It is not yet a goal in this paper to reproduce the real reduction behavior of the furnace, but to present the modeling strategy used to help understanding the furnace operations by adapting the input datas of the model to the observations.

DISCUSSION

This modeling answers some questions :

1. The fluidity of the slag in a fully liquid state cannot explain that 90% of the reduction happen at the top of the

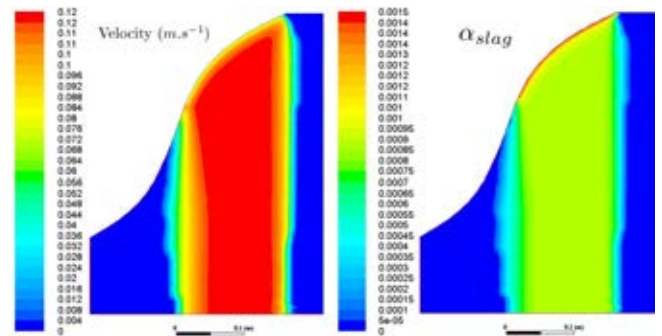


Figure 5: Velocity and phase fraction of the slag phase dripping into the coke bed

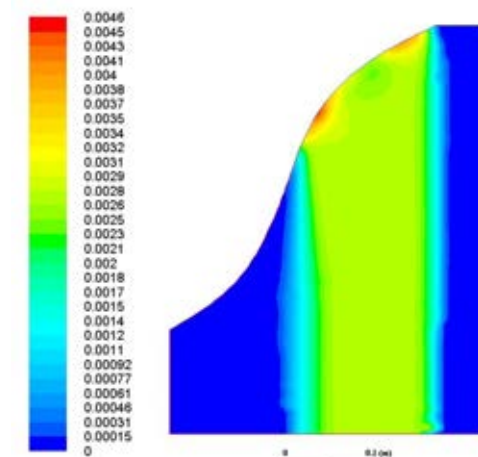


Figure 6: Reaction rate in the coke bed volume ($kmol.m^{-3}.s^{-1}$)

coke bed. Another explanation has to be found to explain the residence time of the slags on this part of the furnace.

2. The slag is not flowing down through the coke bed as a continuous flow but by succession of droplets coming from the reduction zone at the top of the coke bed.
3. The chemical composition of these droplets is not just evolving by reaction along the path imposed to them by the gravity, which would result in very few reduction as their residence time would be small.

Instead, some droplets stay at some places into the coke bed until another droplet push it down. There is certainly a permanent renewal of the chemical concentration of these droplets which are trapped. So it can be considered that a real droplet has an average residence time in the coke bed which is superior to the impression it gives when flowing from cavity to cavity. In addition the renewal of the droplet may depend on the position in the coke bed. On the peripheral part of the main dripping zone, some droplets are renewed less often than in the main flow leading probably to a less important reduction rate. In 3D also there are more accessible places for a droplet to stay before being pushed by another one. In addition, the modification of the chemical composition of the droplets modifies the physical properties. The trajectories of these droplets are very sensible to the physical properties due to the combination of variation of properties as the contact angle, the surface tension and the viscosity. The trajectories of the flow will probably defer from droplet to droplet leading to an exploration of the whole geometry and a lower renewal of droplets trapped in the coke bed, increasing their residence time. However in some conditions, the limited height of the coke bed allow for some droplets to flow without being trapped.

All these considerations can be taken into account in the global modeling by adapting the K_{p-s} drag coefficient to a value consistent with the evaluated residence time in the coke bed. This will be a parameter which will influence the way the reaction rate will be calculated and need to be taken into account.

Here the reduction rate calculated is not in accordance with the real transformation rate. Some thermal datas used are not totally accurate and the real kinetic need to be reformulated with the last datas obtained about the Si-Mn reduction process in order to be compared with a real production rate. In addition the gunn correlation is not well adapted when the liquid is not the continuous phase.

However, the modeling strategy presented here, can give some useful informations about the reality of some hypothesis formulated, and may assess if it is realistic to estimate that 10% of the slag reduction occur in the coke bed.

CONCLUSIONS

A modeling strategy to simulate the behaviour of a Pilot-scale Si-Mn production furnace in relation with experiments analysis has been proposed. For this purpose, a 2D numerical model of the dripping slag across the coke bed zone is detailed.

The developed numerical model is based on two different scales using two different approach of the multiphase modeling.

1. The first one is a detailed model on a small scale aiming at using the fluid properties of the slag to describe how

it can flow into a dry coke bed when traveling from the reduction zone to the bottom of the furnace.

2. The second one use hydrodynamic results of the interaction between the solid phase and the slag phase calculated in the first one to describe the whole geometry with averaged quantities.

The first one use the VOF-isoAdvector method when the other one use the Euler-Euler model. The results show us that the liquid slag is flowing through the coke-bed by a succession of droplet and that the averaged flowing velocity is about 0.12 m/s. The diameter of the droplet cannot be higher than 9-10 mm to avoid their break-up. The residence time of the droplets should be greater than the apparent velocity of the fluid to take into account that the droplets stay often trapped into the coke-bed. These effects can be taken into account into the big scale model by introducing the appropriate drag coefficient. This model can be used to simulate the reductions reaction and validate a thermal balance of the coke bed zone.

ACKNOWLEDGEMENTS

The work reported herein was funded by the Norwegian Research Council through the Centre for Research-Based Innovation Metal Production.

REFERENCES

- DARMANA, D., OLSEN, J., TANG, K. and RINGDALEN, E. (2012). "Modelling concept for submerged arc furnaces". *Ninth International Conference on CFD in the Minerals and Process Industries CSIRO, Melbourne, Australia 10-12 December 2012*. URL http://www.cfd.com.au/cfd_conf12/PDFs/062DAR.pdf.
- HUSSLAG, W.M., BAKKER, T., STEEGHS, A.G.S., REUTER, M.A. and HEEREMA, R.H. (2005). "Flow of molten slag and iron at 1500 c to 1600 c through packed coke beds". *Metallurgical and Materials Transactions B*, **36(6)**, 765–776. URL <http://dx.doi.org/10.1007/s11663-005-0080-6>.
- REMACLE, J.F., HENROTTE, F., CARRIER-BAUDOIN, T., E, B. and MERCHANDISE, E. (2010). "A frontal delaunay quad mesh generator using the linf norm". *Int. J. Numer. Meth. Engng.* URL <http://onlinelibrary.wiley.com/doi/10.1002/nme.4458/abstract>.
- RINGDALEN, E. and TANGSTAD, M. (2013). "Study of simn production in pilot scale experiments". *INFACON*. URL <http://www.pyro.co.za/InfaconXIII/0195-Ringdalen.pdf>.
- ROENBY, J., BREDMOSE, H. and JASAK, H. (2016). "A computational method for sharp interface advection". *Royal Society Open Science*, **3(11)**. <http://rsos.royalsocietypublishing.org/content/3/11/160405.full.pdf>, URL <http://rsos.royalsocietypublishing.org/content/3/11/160405>.